Scilight

Photochemistry and Spectroscopy
https://www.sciltp.com/journals/ps

Article

Check for updates

Electronic Absorption and Vibrational Spectra of Poly(Benzodifurandione) (PBFDO) †

Soichiro Koga and Yukio Furukawa *

Department of Chemistry and Biochemistry, Graduate School of Advanced Science and Engineering, Waseda University, Tokyo 169-8555, Japan
* Correspondence: furukawa@waseda.jp
† This article is dedicated to Prof. Giuseppe Zerbi in recognition of his outstanding scientific contributions to Spectroscopy.

How To Cite: Koga, S.; Furukawa, Y. Electronic Absorption and Vibrational Spectra of Poly(Benzodifurandione) (PBFDO). *Photochemistry and Spectroscopy* **2026**, *2*(2), 4. https://doi.org/10.53941/ps.2026.100015

Received: 29 November 2025
Revised: 27 January 2026
Accepted: 28 January 2026
Published: 20 April 2026

Abstract: We present the UV–Vis–NIR, infrared, and Raman spectra of dedoped neutral PBFDO and redoped PBFDO at various doping levels. The infrared spectrum of a PBFDO film doped at various doping levels showed broad background absorption with many peaks and derivative-like bands. These features were interpreted as the electron–molecular–vibration coupling between broad electronic absorption and discrete vibrational levels and the presence of doping-induced infrared bands associated with the strong Raman bands of neutral PBFDO. The UV–Vis–NIR absorption spectra of doped PBFDO showed two bands at 0.26 and 0.86 eV, which are attributable to negative polarons. No transition from polarons to bipolarons was observed. At the maximum doping level, a polaron network that exhibited metallic properties was likely formed.

Keywords: conducting polymer; PBFDO; polaron; polaron network; UV–Vis–NIR; vibrational spectroscopy

1. Introduction

The 2000 Nobel Prize in Chemistry was awarded to Drs. A. J. Heeger, A. G. MacDiarmid, and H. Shirakawa for the discovery and development of electrically conductive polymers such as polyacetylene, polythiophene, and polypyrrole [1]. They have conjugated π electrons that exhibit semiconductor behavior. When a polymer film is doped with an electron acceptor, such as iodine or $FeCl_3$, or an electron donor, such as Na, it exhibits high electrical conductivity. Upon donor doping, the polymer chains become negatively charged and form complexes with donor cations such as Na^+. Upon acceptor doping, the polymer chains become positively charged and form complexes with dopant anions such as I_3^- or $FeCl_4^-$. Electronic properties such as electrical conductivity can be controlled by the doping level. Undoped polymers are applicable as active materials for displays, sensors, and solar cells. Doped polymers are used as electrodes and coatings. Recently, they have been expected to be used as active materials for flexible thermoelectric generators [2].

There are few n-type conducting polymers, whereas many high-performance p-type conducting polymers have been discovered. Tang et al. [3] reported high-performance n-type PBFDO. PBFDO is synthesized via the oxidative polymerization of 3,7-dihydrobenzo[1,2-b:4,5-b′]difuran-2,6-dione in the presence of tetramethyl-1,4-benzoquinone. In the oxidative polymerization process, tetramethyl-1,4-benzoquinone is reduced to tetramethyldihydroquinone. This compound reduces the resulting polymer. Thus, n-type doped PBFDO is formed. The mechanisms of these reactions were studied using NMR, ESR, MALDI-TOF-MS, IR, and XRD methods. In the doped state, the negative charges generated on the polymer chains are compensated with protons attached to the carbonyl groups, as shown in Figure 1a. A film of n-type doped PBFDO can be prepared from a DMSO solution using the drop-cast method or the spin-cast method. The electrical conductivity of a film at room temperature is more than 2000 S cm^{-1}; the average carrier concentration is estimated to be 1.30×10^{22} cm^{-3} from Hall effect measurements; and the room-

temperature Hall mobility is 1.01 $cm^2V^{-1}s^{-1}$ [3]. XRD measurements revealed that the PBFDO film is crystalline [3]. The electrical conductivity of an unencapsulated doped PBFDO film maintains almost 95% of the initial value after 35 d of exposure to air (25 °C, 60% relative humidity) [3]. PBFDO is very stable in air even in the doped state. A similar polymerization method based on $Cu(OAc)_2$ has also been reported [4]. Dedoping can be performed by treating a doped film with an oxidant agent such as $NOBF_4$ or by an electrochemical method. The chemical structure of the neutral state of PBFDO is shown in Figure 1b. The relationship between the doping level and charge transport properties was investigated [5].

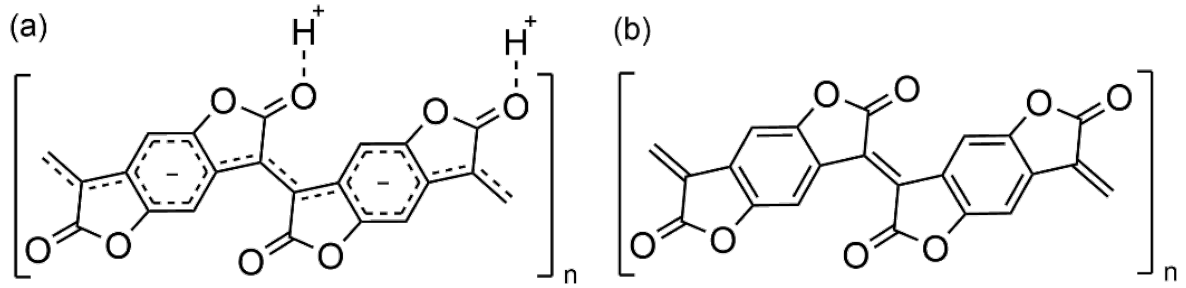

Figure 1. Chemical structure of (**a**) doped and (**b**) neutral PBFDO.

In general, the electronic states of a conducting polymer change upon doping. Upon light doping, localized electronic states associated with a polaron or a bipolaron are formed. These bands can be detected using visible (Vis) and near-infrared (NIR) absorption spectroscopy. Undoped neutral polymers exhibit electronic absorption in the Vis–NIR range. The electronic structures of neutral polymers are interpreted by one-electron theory [6]. In an infinite π-conjugated polymer chain, the valence band (VB) and the conduction band (CB) are formed, as shown in Figure 2a. A band gap and the widths of VB and CB depend on π-conjugated systems. Two kinds of carriers exist in conjugated polymers: singly charged polarons (charge $\pm e$, spin 1/2) and doubly charged bipolarons (charge $\pm 2e$, no spin) [7–9]. Owing to the strong electron–lattice interaction, the charge is localized with structural changes. Two localized electronic levels form at $\pm\varepsilon$ within the bandgap for the polaron (Figure 2b), and at $\pm\varepsilon$' for the bipolaron (Figure 2c). One electron is added to the $+\varepsilon$ level for the polaron, whereas two electrons are added to the $+\varepsilon$' level for the bipolaron. The wavefunctions of these localized states are localized. A negative polaron has the following transitions:

(1) P_1 transition: CB ← $+\varepsilon$ level
(2) P_2 transition: $+\varepsilon$ level ← $-\varepsilon$ level
(3) P_3 transition: $+\varepsilon$ level ← VB and CB ← $-\varepsilon$ level

A negative bipolaron has the following two transitions:

(1) BP_1 transition: CB ← $+\varepsilon$' level
(2) BP_3 transition: CB ← $-\varepsilon$ level

The P_3 transition of the negative polaron and the BP_3 transition of the negative bipolaron are very weak or forbidden. Therefore, negative polarons show two absorption bands from the Vis to the IR range, whereas negative bipolarons show one band [10,11]. These features were demonstrated theoretically even in the presence of electron−electron interactions [12]. Highly or maximally doped polymers exhibit Drude-like absorption extending to the infrared region. However, the electronic structure has not yet been fully elucidated.

The formation of a polaron or bipolaron affects the vibrational states of a polymer. In general, some strong infrared absorption bands are observed upon doping. These doping-induced infrared bands and the Raman spectrum of a neutral polymer have been explained using the effective conjugation coordinate theory proposed by Zerbi and colleagues [13–16]. Raman spectroscopy is useful for identifying the type of carrier [10,11,17–19]. At light and medium doping levels, the electronic states associated with polarons/bipolarons are localized. Thus, the observed macroscopic electrical conductivities are interpreted as variable range hopping (VRH) [20]. At the maximum doping level, a Drude-like absorption extending to the infrared region is observed; this state may be metallic.

The Hall effect is a powerful tool for studying the density of carriers in semiconductors and conductors. In conducting polymers, localized hopping carriers and delocalized band carriers exist. In Hall effect measurements, the Lorentz force acts mainly on band carriers that have microscopic drift velocities; these band carriers contribute to the Hall voltage, whereas hopping carriers do not [21,22]. In this case, Hall effect measurements overestimate the carrier density and underestimate the carrier mobility, which is called the "improper" Hall effect [21]. The Hall effect of conducting polymers have been measured [23–31]. Improper Hall effect measurements have also been

reported [23–25,27,28,31]. Recently, we developed an analytical method for resolving the improper Hall effect [31] using the theory reported by Yi et al. [21]. Regardless, the observation of the Hall effect probably shows the presence of band carriers in conducting polymers. Thus, the Hall effect affords a key to an understanding of the electronic structures of conducting polymers.

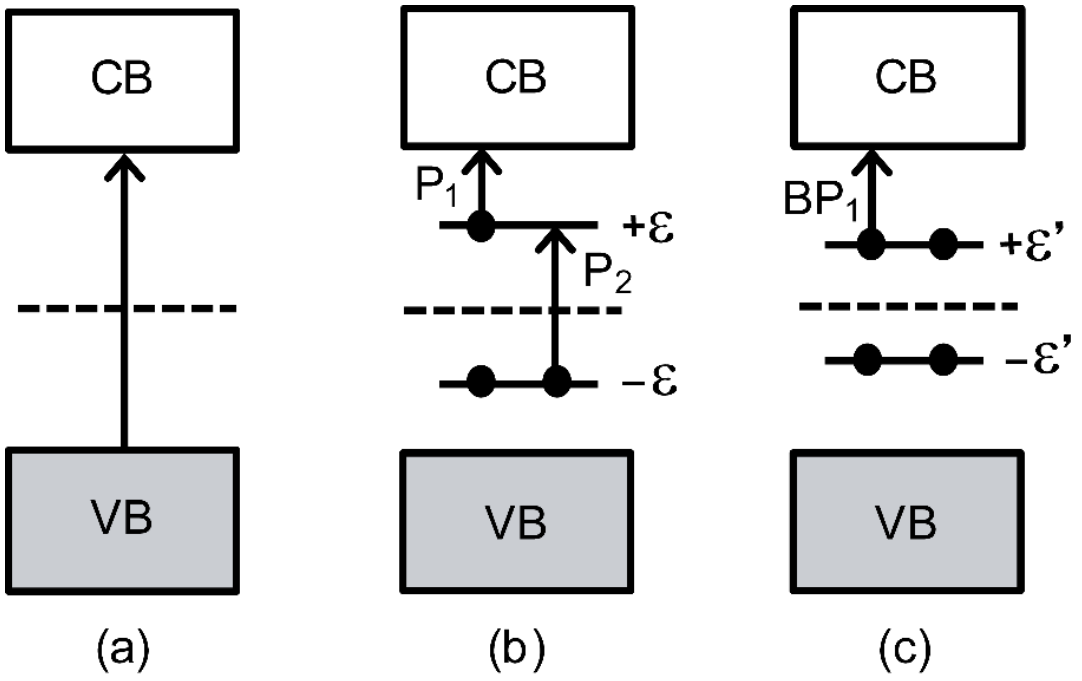

Figure 2. Schematic electronic structures of (**a**) a neutral polymer; (**b**) a negative polaron; and (**c**) a negative bipolaron. CB, conduction band; VB, valence band.

This paper describes an analysis of the vibrational spectra and optical absorption spectra of PBFDO doped at various levels. We discuss the energy band structure of maximally doped PBFDO from optical absorption and the Hall effect. We conclude that a half-filled energy band is formed.

2. Materials and Methods

PBFDO was synthesized by the oxidative polymerization of 3,7-dihydrobenzo[1,2-b:4,5-b′]difuran-2,6-dione (Tokyo Chemical Industry Co. (Tokyo, Japan), Purity > 98.0%) in the presence of tetramethyl-1,4-benzoquinone (Tokyo Chemical Industry Co. (Tokyo, Japan), Purity > 98.0%) according to a previous paper [3]. A film of doped PBFDO was prepared from a DMSO solution of doped PBFDO by the spin-coating method. The film thickness, measured using a Dektak XT-S stylus profiler (Bruker Co., Billerica, MA, USA), was 89 ± 6 nm. The film was heated at 80 °C for 10 min in the air. The doped PBFDO film was converted to a neutral PBFDO film by immersing the film into a 36 mmol L^{-1} acetonitrile solution of $NOBF_4$ (FUJIFILM Wako Pure Chemical Co. (Osaka, Japan) purity > 95%). Hydrazine monohydrate (FUJIFILM Wako Pure Chemical Co. (Osaka, Japan) purity: 98.0%) was dissolved in ethanol. The neutral PBFDO film was redoped at various doping levels by immersing the film into a solution of hydrazine (0.5 mmol L^{-1}) for 5 s, 15 s, 25 s, and 1 min; the maximum amount of doping was achieved by immersing the film into a solution of hydrazine (4 mmol L^{-1}) for an additional 5 min. The UV–Vis–NIR spectra were measured on a JASCO V-570 UV/Vis/NIR spectrometer (JASCO Corp., Hachioji, Japan). IR spectra were measured on a JASCO FT/IR-6800 FT-IR spectrometer. Raman spectra were measured on a RENISHAW InVia Raman microscope (Renishaw plc, Wotton-under-Edge, UK). The excitation wavelength was 830 nm. The DC electrical conductivity and Hall effect measurements were performed using a ResiTest 8400 (TOYO Co., Tokyo, Japan) system in the van der Pauw configuration at 302 K. The thickness of the sample film used for the measurements was 1.00×10^2 nm.

3. Results and Discussion

3.1. Infrared and Raman Spectra of Neutral PBFDO

The vibrational spectra of PBFDO are assigned on the basis of the infinite planar structure, which has a repeating unit $C_{10}H_2O_4$. The vibrational irreducible representation at the zone center (k = 0) of a planar infinite

polymer chain (C_{2h}) is as follows: 16Ag + 7Au + 7Bg + 14Bu. The Ag and Bg modes are Raman-active, whereas the Au and Bu modes are infrared-active. The Ag and Bg modes are in-plane vibrations, whereas the Au and Bg modes are out-of-plane vibrations. The infrared absorption and Raman spectra are shown in Figure 3a,b, respectively. The strong Raman bands at 1753, 1505, 1286, 1240, 1142, 1068, 962, 738, 703, 467, 387, and 249 cm^{-1} are assigned to the Ag symmetry species. The 1753-cm^{-1} Raman band is assigned to the C=O stretching vibration (Ag). The 1777-cm^{-1} infrared band is assigned to the C=O stretching vibration (Bu); this wavenumber value is characteristic of the five-member lactone ring [32]. The strongest infrared band at 1076 cm^{-1} is attributable to the C−O stretching vibration (Bu).

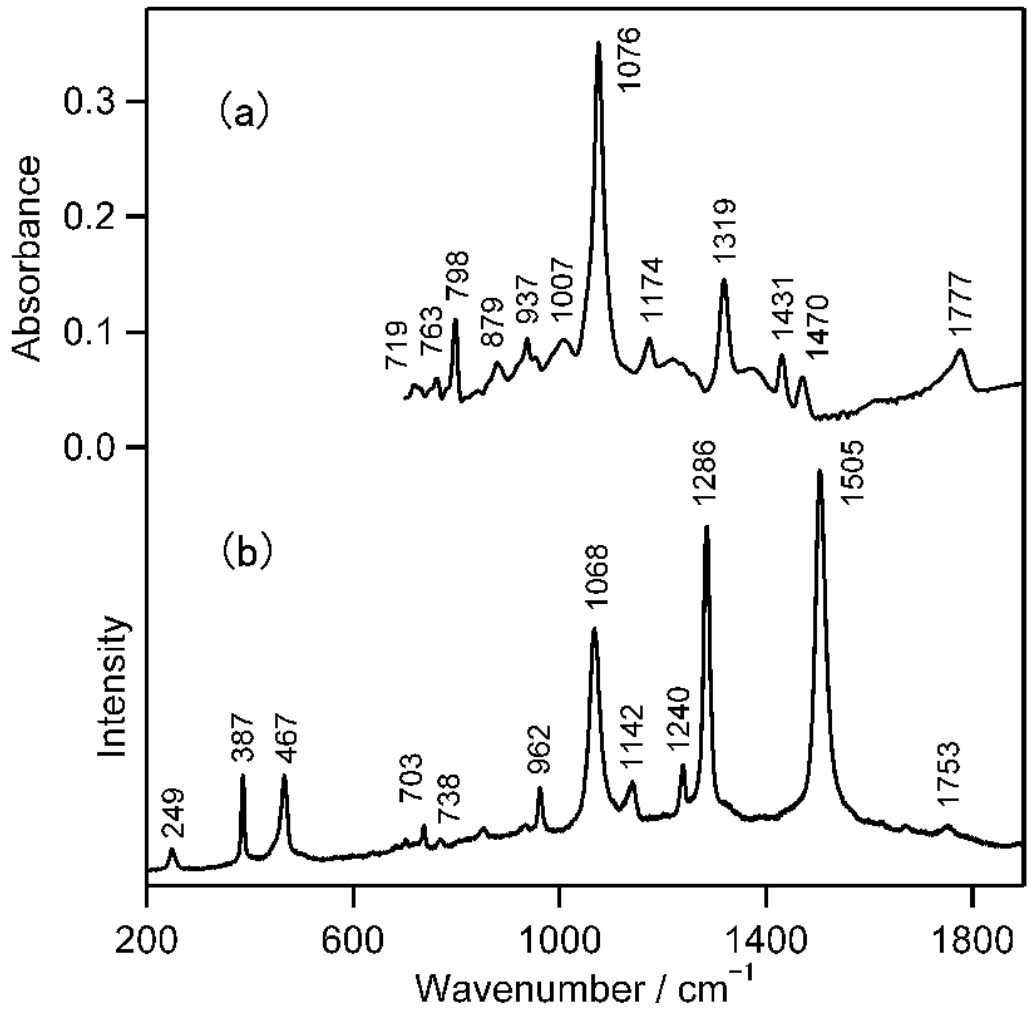

Figure 3. (**a**) Infrared absorption and (**b**) Raman spectra of a neutral PBFDO film. The excitation wavelength of the Raman spectrum is 830 nm.

3.2. Doping-Induced Infrared Absorption

The infrared absorption spectra of a PBFDO film doped at various levels are shown in Figure 4. Spectrum (a) shows the infrared spectrum of the dedoped neutral PBFDO film. The doping level increases from (b) to (f); (f) is the spectrum of the maximum doping. In the spectra from (b) to (f), a broad band is observed in the whole range; many peaks and derivative-like bands are also observed. These spectral features are characteristic of electron–molecular-vibration (EMV) coupling, which is the interaction between a broad electronic band and discrete levels due to molecular vibrations [33–35]. Broad bands with small peaks are observed at approximately 1365, 1190, and 940 cm^{-1}. These bands are likely attributable to doping-induced infrared absorption bands. In some review papers concerning doping-induced infrared absorption bands [14,15,18], iodine-doped polyacetylene exhibits bands at 1398, 1290, and 886 cm^{-1}; iodine-doped polythiophene bands at 1327, 1200, 1113, 1026, 785 cm^{-1}, etc. No small peaks and no derivative-like bands are observed. According to the effective conjugation coordinate theory [13–16], the doping-induced bands at approximately 1365, 1190, and 940 cm^{-1} correspond to the strong Raman bands at 1505, 1286, and 1068 cm^{-1}, respectively. The observed infrared features are quite different from those reported for most conducting polymers.

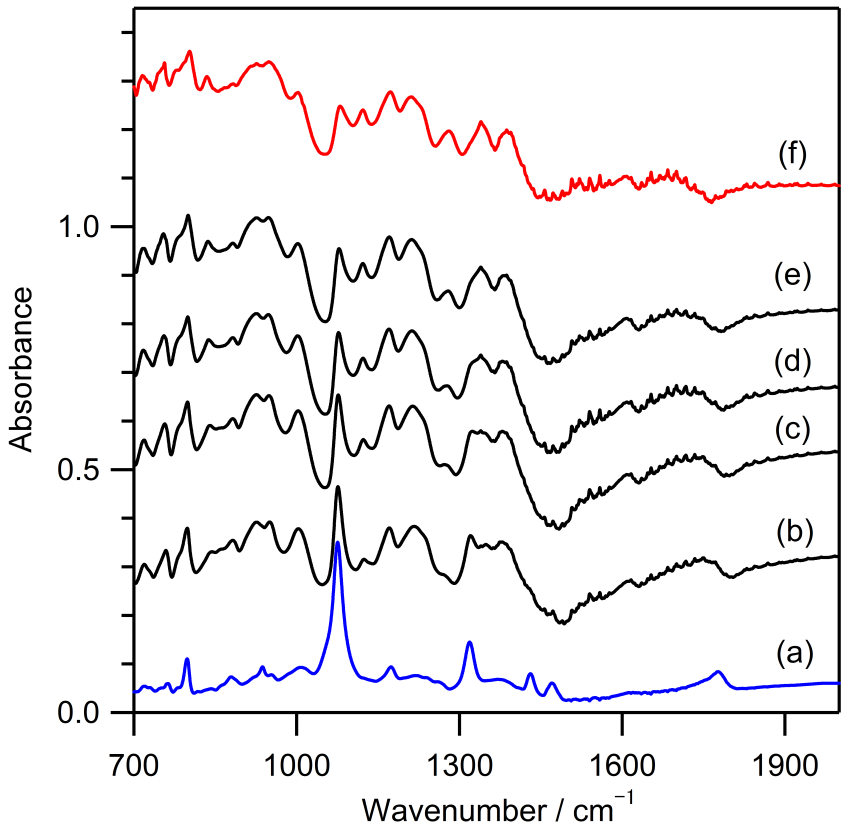

Figure 4. Infrared spectra of a PBFDO film at various doping levels: (**a**) dedoped neutral PBFDO film; (**b**–**f**) redoped film at various levels. The degree of doping increases from (**b**) to (**f**); (**f**) is the maximum degree of doping.

3.3. Optical Absorption Spectra at Various Doping Levels

The optical absorption spectra of PBFDO at various doping levels are shown in Figure5. In the spectrum of neutral PBFDO (Figure 5a), two absorption peaks are observed at 1.42 and 2.49 eV, which are due to π–π* transitions [36]. The 1.42 eV band is dominated by the HOMO → LUMO transition [36]. At the initial stage of doping (Figure 5b), new broad bands appeared at 0.26 and 0.86 eV. The 0.26-eV and 0.86-eV bands are attributed to the P_1 and P_2 transitions of negative polarons, respectively. As the doping level increases, these two bands become strong monotonically. At the maximum doping level (Figure 5f), these two peaks are not clear; a Drude-like absorption extending to the infrared region is observed. Notably, a change from polarons to bipolarons was not observed. On the other hand, bipolarons are stable in polythiophene and its derivatives. A transition from polarons to bipolarons was reported for the doping-dependent optical spectrum of poly(2,5-bis(3-hexadecylthiophene-2-yl)thieno[3,2-b]thiophene) (PBTTT-C16) [37]. We observed the Hall coefficient of the maximally doped PBFDO film. The measured Hall coefficient was -4.44×10^{-4} cm^3 C^{-1}. The charge number density was calculated to be 1.41×10^{22} cm^{-3}. The sign of the carrier was negative. The electrical conductivity was 1.33×10^3 S cm^{-1}. The Hall mobility was calculated to be 0.590 cm^2 V^{-1} s^{-1}. Notably, the observation of the Hall effect indicates that a band is formed at the maximum doping level.

When the doping level is light and medium, localized electronic levels due to negative polarons are formed within the band gap. The wavefunctions of these electronic states are localized. On the other hand, at the maximum doping level, many polarons are formed and form a polaron network [38]. In the network, the localized wavefunctions of many polaron levels interact with each other to generate delocalized electronic states, HPB and LPB bands shown in Figure 6. The electronic configuration of a negative polaron is shown in Figure 6a. The 0.26-eV and 0.86-eV bands were assigned to the P_1 and P_2 transitions, respectively. The energy difference between the bottom of CB and the $+\varepsilon$ level is 0.26 eV. The energy difference between the $+\varepsilon$ and $-\varepsilon$ levels is 0.86 eV. The $-\varepsilon$ level is formed symmetrically against the center of the bandgap. The energy difference between the $-\varepsilon$ level and the top of VB is 0.26 eV. Thus, the bandgap is calculated to be 1.38 eV, which is quite similar to an experimental value 1.3 eV reported in Ref. [4]. In the electronic configuration of the polaron network (Figure 6b), a half-filled metallic band, HPB, is formed from the $+\varepsilon$ levels of many polarons. Thus, the metallic properties of PBFDO can be interpreted by the polaron network.

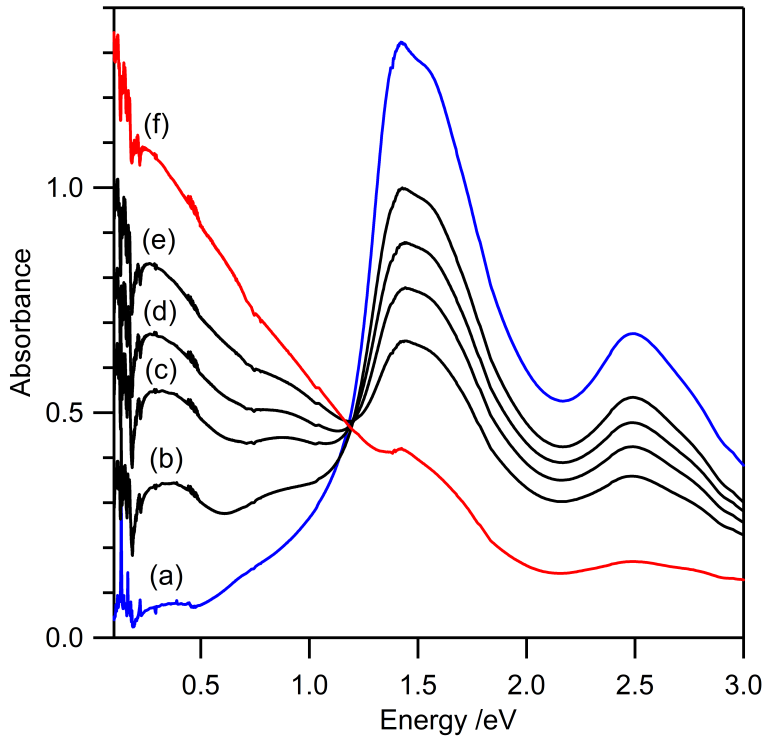

Figure 5. Optical absorption spectra of a PBFDO film at various doping levels: (**a**) neutral PBFDO; the doping level increases from (**b**) to (**f**); (**b**–**f**) redoped film at various levels. (**f**) the maximum doping level.

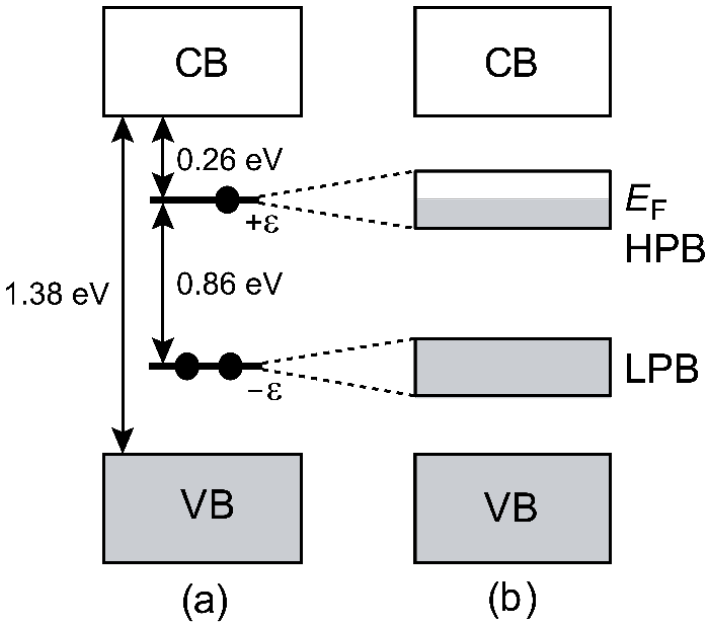

Figure 6. Schematic electronic structures of (**a**) a negative polaron and (**b**) a polaron network: VB, valence band; CB, conduction band; LPB, lower polaron band; HPB, higher polaron band; E_F, the Fermi level.

4. Conclusions

Infrared and Raman spectra of dedoped neutral poly(benzodifurandione) (PBFDO) were studied. The infrared spectra of a PBFDO film doped at various levels showed broad electronic absorption with many peaks and derivative-like bands associated with discrete vibrational levels, which were interpreted as electron–molecular–vibration coupling and doping-induced infrared bands that correspond to strong Raman bands. The UV–Vis–NIR absorption spectra of the PBFDO film doped at various levels showed two bands at 0.26 and 0.86 eV, which are attributable to negative polarons. No transition from polarons to bipolarons was observed. At the maximum doping level, a polaron network that exhibited metallic properties was likely formed.

Author Contributions

S.K.: investigation, data curation, writing—original draft. Y.F.: investigation, writing—review & editing, conceptualization, project administration. Both authors have read and agreed to the published version of the manuscript.

Funding

This research received no external funding.

Institutional Review Board Statement

Not applicable.

Informed Consent Statement

Not applicable.

Data Availability Statement

Data will be made available on request.

Conflicts of Interest

The authors declare no conflict of interest.

Use of AI and AI-Assisted Technologies

No AI tools were utilized for this paper.

References

1. The Nobel Prize in Chemistry 2000. Available online: https://www.nobelprize.org/prizes/chemistry/2000/summary/ (accessed on 5 February 2026).
2. Zhao, W.; Ding, J.; Zou, Y.; et al. Chemical Doping of Organic Semiconductors for Thermoelectric Applications. *Chem. Soc. Rev.* **2020**, *49*, 7210–7228.
3. Tang, H.; Liang, Y.; Liu, C.; et al. A Solution-Processed N-Type Conducting Polymer with Ultrahigh Conductivity. *Nature* **2022**, *611*, 271–277.
4. Ke, Z.; Abtahi, A.; Hwang, J.; et al. Highly Conductive and Solution-Processable N-Doped Transparent Organic Conductor. *J. Am. Chem. Soc.* **2023**, *145*, 3706–3715.
5. Cui, W.; Jiang, Q.; He, X.; et al. Charge Transport Properties of PBFDO at Various Doping Levels: An Electrochemical Control and Hall Effect Characterization Study. *J. Phys. Chem. Lett.* **2025**, *16*, 6393–6401.
6. Fesser, K.; Bishop, A.R.; Campbell, D.K. Optical Absorption from Polarons in a Model of Polyacetylene. *Phys. Rev. B* **1983**, *27*, 4804–4825.
7. Brazovskiĭ, S.A.; Kirova, N.N. Excitons, Polarons, and Bipolarons in Conducting Polymers. *JETP Lett.* **1981**, *33*, 6–10.
8. Bishop, A.R.; Campbell, D.K.; Fesser, K. Polyacetylene and Relativistic Field Theory Models. *Mol. Cryst. Liq. Cryst.* **1981**, *77*, 253–264.
9. Brédas, J.L.; Chance, R.R.; Silbey, R. Theoretical Studies of Charged Defect States in Doped Polyacetylene and Polyparaphenylene. *Mol. Cryst. Liq. Cryst.* **1981**, *77*, 319–332.
10. Furukawa, Y. Electronic Absorption and Vibrational Spectroscopies of Conjugated Conducting Polymers. *J. Phys. Chem.* **1996**, *100*, 15644–15653.
11. Yamamoto, J.; Furukawa, Y. Electronic and Vibrational Spectra of Positive Polarons and Bipolarons in Regioregular Poly(3-hexylthiophene) Doped with Ferric Chloride. *J. Phys. Chem. B* **2015**, *119*, 4788–4794.
12. Shimoi, Y.; Abe, S.; Harigaya, K. Theory of Optical Absorption in Doped Conjugated Polymers. *Mol. Cryst. Liq. Cryst.* **1995**, *267*, 329–336.
13. Castiglioni, C.; Navarrete, J.T.L.; Zerbi, G.; et al. A Simple Interpretation of the Vibrational Spectra of Undoped, Doped and Photoexcited Polyacetylene: Amplitude Mode Theory in the GF Formalism. *Solid State Commun.* **1988**, *65*, 625–630.
14. Gussoni, M.; Castiglioni, C.; Zerbi, G. Vibrational Spectroscopy of Polyconjugated Materials: Polyacetylene and Polyenes. In *Spectroscopy of Advanced Materials*; Clark, R.J.H., Hester, R.E., Eds.; John Wiley & Sons: Chichester, UK, 1991; pp. 251–353.

15. Gussoni, M.; Castiglioni, C.; Zerbi, G. Vibrational Spectroscopy of Polyconjugated Aromatic Materials with Electrical and Non Linear Optical Properties. In *Conjugated Polymers*; Brédas, J.L., Silbey, R., Eds.; Kluwer Academic Publishers: Dordrecht, The Netherlands, 1991; pp. 435–507.
16. Zerbi, G. Vibrational Spectroscopy of Conducting Polymers: Theory and Perspective. In *Vibrational Spectroscopy of Polymers: Principles and Practice*; Everall, N.J., Chalmers, J.M., Griffiths, P.R., Eds.; John Wiley & Sons: Chichester, UK, 2007; pp. 487–536.
17. Furukawa, Y.; Tasumi, M. Vibrational Spectroscopy of Intact and Doped Conjugated Polymers and Their Models. In *Modern Polymer Spectroscopy*; Zerbi, G., Ed.; Wiley-VCH: Weinheim, Germany, 1991; pp. 207–237.
18. Furukawa, Y. Vibrational Spectroscopy of Conducting Polymers: Fundamental and Applications. In *Vibrational Spectroscopy of Polymers: Principles and Practice*; Everall, N.J., Chalmers, J.M., Griffiths, P.R., Eds.; John Wiley & Sons: Chichester, UK, 2007; pp. 537–556.
19. Furukawa, Y. Recent Application of Vibrational Spectroscopy to Conjugated Conducting Polymers. In *Spectroscopic Techniques for Polymer Characterization*; Ozaki, Y., Sato, H., Eds.; Wiley-VCH: Weinheim, Germany, 2022; pp. 367–391.
20. Mott, N.F.; Davis, E.A. *Electronic Processes in Non-Crystalline Materials*, 2nd ed.; Oxford University Press: Oxford, UK, 2012.
21. Yi, H.T.; Gartstein, Y.N.; Podzorov, V. Charge Carrier Coherence and Hall Effect in Organic Semiconductor. *Sci. Rep.* **2016**, *6*, 23650.
22. Chen, Y.; Yi, H.T.; Podzorov, V. High-Resolution AC Measurements of the Hall Effect in Organic Field-Effect Transistors. *Phys. Rev. Appl.* **2016**, *5*, 034008.
23. Kanazawa, K.K.; Diaz, A.F.; Gill, W.D.; et al. Polypyrrole: An Electrochemically Synthesized Conducting Organic Polymer. *Synth. Met.* **1979**, *1*, 329–336.
24. Fukuhara, T.; Masubuchi, S.; Kazama, S. Hall Effect in ClO_4^- Doped Polythiophene and Poly(3-methylthiophene). *Synth. Met.* **1995**, *69*, 359–360.
25. Gilani, T.H.; Ishiguro, T. Low-Temperature Metallic Conductance in PF6-Doped Polypyrrole. *J. Phys. Soc. JPN* **1997**, *66*, 727–732.
26. Wang, S.; Ha, M.; Manno, M.; et al. Hopping Transport and the Hall Effect near the Insulator–Metal Transition in Electrochemically Gated Poly(3-hexylthiophene) Transistors. *Nat. Commun.* **2012**, *3*, 1210.
27. Stadler, P.; Leonat, L.N.; Menon, R.; et al. Stable Hall Voltages in Presence of Dynamic Quasi-Continuum Bands in Poly(3,4-ethylene-dioxythiophene). *Org. Electron.* **2019**, *65*, 412–418.
28. Yoon, S.E.; Park, J.; Kwon, J.E.; et al. Improvement of Electrical Conductivity in Conjugated Polymers through Cascade Doping with Small-Molecular Dopants. *Adv. Mater.* **2020**, *32*, 2005129.
29. Liang, Z.; Choi, H.H.; Luo, X.; et al. N-Type Charge Transport in Heavily P-Doped Polymers. *Nat. Mater.* **2021**, *20*, 518–524.
30. Sato, R.; Wasai, Y.; Izumi, Y.; et al. Influence of Effective Mass on Carrier Concentration for PEDOT:PSS and S-PEDOT Thin Films Studied by Ellipsometry and Hall Measurement. *J. Phys. Chem. C* **2023**, *127*, 13196–13204.
31. Shimokawa, D.; Nishikitani, Y.; Kubo, T.; et al. Hall Effect Analysis of Conducting Polymers Doped Poly(3,4-ethylenedioxythiophene) (PEDOT) Using Band and Hopping Transport Mechanisms. *Synth. Met.* **2025**, *314*, 117942.
32. Larkin, P.J. *IR and Raman Spectroscopy*; Elsevier: Amsterdam, The Netherlands, 2011; p. 100.
33. Rice, M.J.; Lipari, N.O.; Strässler, S. Dimerized Organic Linear-Chain Conductors and the Unambiguous Experimental Determination of Electron–Molecular-Vibration Coupling Constants. *Phys. Rev. Lett.* **1977**, *39*, 1359–1362.
34. Bozio, R.; Zanon, I.; Girlando, A.; et al. Vibrational Spectroscopy of Molecular Constituents of One-Dimensional Organic Conductors. Tetrathiofulvalene (TTF), TTF^+, and $(TTF^+)_2$ Dimer. *J. Chem. Phys.* **1979**, *71*, 2282–2289.
35. Imamura, T.; Funatsu, K.; Ye, S.; et al. Coupling of Ground-State Molecular Vibrations to Low-Energy Electronic Transitions of Ruthenium(III, II) Porphin Dimers. *J. Am. Chem. Soc.* **2000**, *122*, 9032–9037.
36. Li, N.; Sheng, H.; Sun, Y.; et al. Spectroscopic Study on Size-Dependent Optoelectronics of N-Type Ultra-High Conductive Polymer PBFDO. *Spectrochim. Acta, Part A* **2023**, *298*, 122744.
37. Enokida, I.; Furukawa, Y. Doping-Level Dependent Mobilities of Positive Polarons and Bipolarons in Poly(2,5-bis(3-hexadecylthiophen-2-yl)thieno[3,2-b]thiophene) (PBTTT-C16) Based on an Ionic-Liquid-Gated Transistor Configuration. *Org. Electron.* **2019**, *68*, 28–33.
38. Bubnova, O.; Khan, Z.U.; Wang, H.; et al. Semi-Metallic Polymers. *Nat. Mater.* **2014**, *13*, 190–194.